XXXVI Ibero-Latin American
Congress on Computational
Methods in Engineering
CILAMCE
Rio de Janeiro, 22-25 Nov 2015

MESHFREE FINITE ELEMENT TECHNIQUES USING NOVEL FAMILIES OF COMPACTLY SUPPORTED RADIAL BASIS FUNCTIONS

Fernando César Meira Menandro

Wesley Ferrari

Nikolas Garcia Repsold

menandro@ct.ufes.br

wesleyferrari14@gmail.com

nikolas_rep@hotmail.com

Departamento de Engenharia Mecânica, Centro Tecnolgico, Universidade Federal do Esprito Santo

Av. Fernando Ferrari, 514, 29.075-910, Vitória, Espírito Santo, Brazil

The use of compactly supported radial basis functions (CSRBF) has spread into the scientific approximation community for their localization properties and their mathematical simplicity, since they just depend on a single variable (radius) and, unless the radial basis is not compactly supported, affect the results only on a neighbourhood (support) of the given center (Iske, 2004; Fasshauer, 2007). However, the mathematical derivation of continuous functions for different continuity requirements can be quite cumbersome (Wendland, 2005). In this paper, two new families of CSRBFs are presented for which the continuity requirements are greatly simplified. The first function family proposed consists of a combination of different inverse functions, similar to inverse quadric functions, and is thus called inverse family. The second family is called the rational family, in which the functions are obtained as a ratio of two polynomial functions. The proposed functions are used on a meshfree finite element software which takes advantage of their simplicity. The results seem to demonstrate the accuracy and convergence of the proposed functions when compared to some CSRBFs presented on the subject literature(Menandro et al., 2011).

Keywords: *Compactly supported radial basis functions, Meshfree finite element methods, Least squares methods, non-polynomial radial basis functions)*

1 INTRODUCTION

The use of compactly supported radial basis functions (CSRBF) has spread into the scientific approximation community for their localization properties and their mathematical simplicity, since they just depend on a single variable (radius) and, unless the radial basis is not compactly supported, affect the results only on a neighbourhood (support) of the given center (Iske, 2004; Fasshauer, 2007). For the past two decades the applications have sprung and research has been promising on the use of polynomial radial basis functions (RBF) on compact support. The mathematical derivation of such RBFs is, though, quite elaborate, as can be seen on Wendland (2005), Hubert (2012) and Zhu (2012).

In this paper two novel classes of CSRBFs are presented, which can be used both for approximation of unknown functions and for solution of differential equations, though here only the latter is demonstrated. These two new classes take advantage on a very simple construction rule that guarantees their continuity. A few of these functions are then tested against a few of the well accepted literature functions.

First, a very thorough review of CSRBF literature is conducted, to justify the novelty claim. Then the development of the novel classes is presented.

To test the new classes a two-dimensional heat conduction problem is solved by a meshfree finite element software which uses a discrete least squares residual procedure (Menandro et al., 2011) and a Lagrange multiplier boundary condition enforcement. The results are compared.

Finally, the proposed functions are established as two new classes, and some of the following research challenges on the application of such CSRBFs are outlined.

2 RADIAL BASIS FUNCTIONS REVIEWED

Let $\mathbb{R}^+ = \{x \in \mathbb{R}, x \geq 0\}$ be the set of non-negative numbers, and let $f : \mathbb{R}^+ \to \mathbb{R}$ be a continuous function such that $f(0) \geq 0$. The radial basis function (RBF) $\mathbb{R}$ is the function such that (Goldberg et al., 1999)

$$f(||\mathbf{P} - \mathbf{Q}||), \tag{1}$$

where $(\mathbf{P}, \mathbf{Q}) \in \mathbb{R}^n$ and $||.||$ denotes the euclidean distance between $\mathbf{P}$ and $\mathbf{Q}$, i.e.

$$r = ||\mathbf{P} - \mathbf{Q}|| = \left[(\mathbf{P} - \mathbf{Q}) \cdot (\mathbf{P} - \mathbf{Q})\right]^{1/2}. \tag{2}$$

If one chooses m points $\mathbf{Q}_j$, for $j = 1, m$, m real coefficients a_j can be found such that the linear combination

$$g(\mathbf{P}) = \sum_{j-1}^{m} a_j f(||\mathbf{P} - \mathbf{Q}_j||) \tag{3}$$

interpolates the given function. Function g can also be called a RBF (Goldberg et al., 1999), though it is preferred linear combination of approximating RBFs.

Classical RBFs (Floater and Iske, 1996; Hickernell and Hon, 1999; de Boer et al., 2007), which return non-zero values for $r < \infty$, that is, with infinite support, are:

Duchon's Thin Plate splines,

$$f(r) = r^2 log(r), \tag{4}$$

Hardy's Multiquadrics function,

$$f(r) = (c^2 + r^2)^{1/2}, \tag{5}$$

Inverse Multiquadrics,

$$f(r) = (c^2 + r^2)^{-1/2}, \tag{6}$$

Gaussian,

$$f(r) = e^{-r^2}, \tag{7}$$

Quadrics,

$$f(r) = 1 + r^2, \tag{8}$$

and Inverse Quadrics,

$$f(r) = \frac{1}{1 + r^2}. \tag{9}$$

Due to the infinite support of the classical RBFs, any interpolation routine would behave as a field problem, without localization characteristics, returning full matrices for inversion. This is rather time consuming, and sparked the proposition of functions with local domain. The proposed function should vanish for r greater than a given measure (from now on called support radius or simply support). This function is called a Compactly Supported Radial Basis Function (CSRBF), several of which can be found on the literature. The first CSRBFs to be mentioned are those proposed by Buhmann (1998):

$$f(r) = \begin{cases} \frac{1}{3} + r^2 - \frac{4}{3}r^3 + 2r^2 log(r) & for \;\; 0 \leq r \leq 1, \\ 0 & otherwise, \end{cases} \tag{10}$$

and

$$f(r) = \begin{cases} \frac{1}{15} + \frac{19}{6}r^2 - \frac{16}{3}r^3 + 3r^4 - \frac{16}{15}r^5 + \frac{1}{6}r^6 + 2r^2 log(r) & for \;\; 0 \leq r \leq 1, \\ 0 & otherwise. \end{cases} \tag{11}$$

All CSRBFs present the characteristics of both equations above (10 and 11), in which the behaviour is different if the radius is smaller or greater than the support radius (in this case unity). It is easy to scale the functions such that the unity radius can represent accurately the behaviour of any function within a given family. All CSRBFs described further will be evaluated only for $r \leq 1$, vanishing for $r > 1$.

Wendland (1995) proposed polynomial CSRBFs of minimal degree:

$$f(r) = (1 - r), \tag{12}$$
$$f(r) = (1 - r)^3(3r + 1), \tag{13}$$
$$f(r) = (1 - r)^5(8r^2 + 5r + 1), \tag{14}$$
$$f(r) = (1 - r)^2, \tag{15}$$
$$f(r) = (1 - r)^4(4r + 1), \tag{16}$$
$$f(r) = (1 - r)^6(35r^2 + 18r + 3) \tag{17}$$
$$f(r) = (1 - r)^8(32r^3 + 25r^2 + 8r + 1), \tag{18}$$
$$f(r) = (1 - r)^3, \tag{19}$$
$$f(r) = (1 - r)^5(5r + 1), \tag{20}$$
$$f(r) = (1 - r)^5(16r^2 + 7r + 1). \tag{21}$$

The continuity and positive definiteness of such functions, as proven in Wendland (1995, 1996, 2005), are shown at Table 1:

Table 1: Continuity and spatial dimensions of Wendland polynomial functions.

Function	C^n	Positive Definite
12	C^0	$\mathbb{R}$
13	C^2	$\mathbb{R}$
14	C^4	$\mathbb{R}$
15	C^0	$\mathbb{R}^3$
16	C^2	$\mathbb{R}^3$
17	C^4	$\mathbb{R}^3$
18	C^6	$\mathbb{R}^3$
19	C^0	$\mathbb{R}^5$
20	C^2	$\mathbb{R}^5$
21	C^4	$\mathbb{R}^5$

The paper by de Boer et al. (2007, p.786) also mentions some CSRBFs proposed by Wendland (1996), the first of which are ”thin plate like” functions:

$$f(r) = (1 - r)^5, \tag{22}$$
$$f(r) = 1 + \frac{80}{3}r^2 - 40r^3 + 15r^2 + \frac{8}{3}r^5 + 20r^2 log(r), \tag{23}$$
$$f(r) = 1 - 30r^2 - 10r^3 + 45r^4 - 6r^5 - 60r^3 log(r), \tag{24}$$
$$f(r) = 1 - 20r^2 + 80r^3 - 45r^4 - 16r^5 + 60r^4 log(r). \tag{25}$$

The paper written by Wong et al. (2002, p.84) also includes higher order Wendland functions:

$$f(r) = (1-r)^{10}(429r^4 + 450r^3 + 210r^2 + 50r + 5), \tag{26}$$
$$f(r) = (1-r)^{12}(2048r^5 + 2697r^4 + 1644r^3 + 566r^2 + 108r + 9), \tag{27}$$

The continuity and positive definiteness of the functions above is shown at Table 2. There are two possible C^2 continuous solutions for thin plate like functions that are positive definite in R^3 space.

Table 2: Continuity and spatial dimensions of other Wendland functions.

Function	C^n	Positive Definite
22	C^0	$\mathbb{R}^3$
23	C^4	$\mathbb{R}^3$
24	C^2	$\mathbb{R}^3$
25	C^2	$\mathbb{R}^3$
26	C^8	$\mathbb{R}^3$
27	C^{10}	$\mathbb{R}^3$

Wu (1995), on the other hand, also proposed different minimal degree polynomials:

$$f(r) = (1-r), \tag{28}$$
$$f(r) = (1-r)^3(3r+1), \tag{29}$$
$$f(r) = (1-r)^5(8r^2 + 5r + 1), \tag{30}$$
$$f(r) = (1-r)^2, \tag{31}$$
$$f(r) = (1-r)^4(4r+1), \tag{32}$$
$$f(r) = (1-r)^6(35r^2 + 18r + 3), \tag{33}$$
$$f(r) = (1-r)^6(35r^2 + 18r + 3), \tag{34}$$

for which Table 3 shows continuity and positive definiteness.

Some CSRBFs used in meshless finite element methods and on the Smooth Particle Hydrodynamics method (Belytschko et al., 1996) can also be mentioned, such as the exponential (still $f(r) = 0$ for $r > 1$):

$$f(r) = e^{-(r/\alpha)}, \tag{35}$$

The cubic spline:

$$f(r) = \begin{cases} \frac{2}{3} - 4r^2 + 4r^3, & for \;\; r \leq \frac{1}{2}, \\ \frac{4}{3} - 4r + 4r^2 - \frac{4}{3}r^3, & for \;\; \frac{1}{2} < r \leq \frac{1}{2}, \end{cases} \tag{36}$$

Table 3: Continuity and spatial dimensions of Wu functions.

Function	C^n	Positive Definite
28	C^4	$\mathbb{R}$
29	C^2	$\mathbb{R}^3$
30	C^0	$\mathbb{R}^5$
31	C^4	$\mathbb{R}^3$
32	C^4	$\mathbb{R}^5$
33	C^2	$\mathbb{R}^7$
34	C^0	$\mathbb{R}^9$

or the quadric spline:

$$f(r) = 1 - 6r^2 + 8r^3 - 3r^4. \tag{37}$$

There are also the so called Euclid's Hat functions (Fasshauer, 2007; Schaback, 1995), which can be obtained as in the references. Some of these functions are shown at Equations 38 to 42:

$$\psi_1(r) = 1 - r, \tag{38}$$

$$\psi_2(r) = \frac{2}{\pi}\left(arccos(r) - r\sqrt{1-r^2}\right), \tag{39}$$

$$\psi_3(r) = 1 - \frac{1}{4\pi}\left((1+4\pi)r - r^3\right), \tag{40}$$

$$\psi_4(r) = \frac{2}{\pi}arccos(r) - \frac{1}{2\pi}r(5-r^2)\sqrt{1-r^2}, \tag{41}$$

$$\psi_5(r) = 1 - \frac{1}{8\pi^2}\left((3+2\pi+8\pi^2)r - (3+2\pi)r^3\right). \tag{42}$$

Note that all ϕ_s are strictly positive definite on $\mathbb{R}^s$, but all are only continuous without derivative continuity (C^0).

Quite a few functions were also developed as covariance functions for application on geodesics. Some of them will be mentioned, such as those due to Gaspari and Cohn (1999), who proposed CSRBFs to approximate the first three autoregressive covariance functions: Gaussian and the second and third order Markov models (Moreaux, 2008). The actual description of such functions is quite elaborate and will be left to the reader. Another kind of radial covariance functions are those due to Gneiting (2002). Fasshauer (2007, p.91) describes those functions:

$$\tau_{s,l}(r) = (1-r)^l(1 + lr - \frac{(l+1)(l+2+s)}{s}r^2), \tag{43}$$

which are C^2 continuous and strictly positive definite and radial on $\mathbb{R}^s$ provided $l \geq (s+5)/2$.

From all the literature reviewed, the only rational function mentioned was the Non-Uniform Radial Rational B-Spline, proposed by Schaback (1995, p.12):

$$f(r) = \begin{cases} (85 - 720x^2 + 3528x^4 - 3780x^5 & \\ \qquad -960x^6 + 2160x^7 + 192x^9)/85 & for\ \ 0 \leq r \leq 1/2, \\ 4(x-1)^6(16x^4 + 96x^3 + 156x^2 + 56x - 9)/(85x) & for\ \ 1/2 \leq r \leq 1, \\ 0 & otherwise, \end{cases} \tag{44}$$

There are other functions proposed that are radial, positive definite, and do not vanish only for a distance less than a support radius, but the functions presented here are, by far, the most cited among them. As mentioned on the previous paragraph, none of them was assembled as an inverse polynomial function or as a polynomials ratio. This sparked our interest in investigating the properties of such functions.

3 NOVEL CLASSES OF FUNCTIONS

3.1 Inverse Functions

Inverse functions are composed by a linear combination of inverse polynomials. To facilitate the reference, the ”order” of the function will be the order of the dividing polynomial. In this section different combinations will be attempted to assure continuity of the RBFs and their derivatives at the center and at the support radius (hereupon fixed as one, for ease of writing, without generality prejudice).

The inverse functions will always be constructed from the general formula:

$$I_N(r) = \sum_{i=0}^{N} c_i \frac{1}{1+r^i}. \tag{45}$$

First Inverse Function

The first inverse function to be proposed is:

$$I_1(r) = \frac{c_1}{1+r} - \frac{c_0}{2}. \tag{46}$$

To assure that the proposed function can serve well in the representation of continuous functions at $r = 1$, the function will have to obey the following conditions: $F(0) = 1$, and $F(1) = 0$.

$$\begin{cases} c_1 + \frac{c_0}{2} = 1, \\ \frac{c_1}{2} + \frac{c_0}{2} = 0. \end{cases} \tag{47}$$

As a result the coefficients are found to be $c_0 = -2$ and $c_1 = 2$. Rewriting Eq. 46:

$$I_1(r) = \frac{2}{1+r} - 1. \tag{48}$$

Function I_1 is presented at Figure 1.

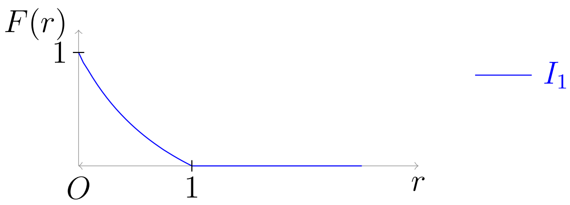

Figure 1: Graphical Representation of function I_1.

The second inverse function presents itself differently, since the continuity of the derivative could either be enforced at the center or at the support radius. For the sake of brevity, its derivation will not be undertaken here.

Third Inverse Function

The third proposed inverse function, which will be one of our test functions, is:

$$I_3(r) = \frac{c_3}{1+r^3} + \frac{c_2}{1+r^2} + \frac{c_1}{1+r} + \frac{c_0}{2}. \tag{49}$$

Once more, to assure that the proposed function can serve well in the representation of continuous functions at $r = 1$, the function will have to obey the following conditions: $I_3(0) = 1$, $I_3(1) = 0$, and two extra conditions regarding the first derivative, which should vanish for both $r = 0$ and $r = 1$.

The first derivative of I_3 is:

$$\frac{dI_3}{dr} = -\frac{3c_3r^2}{(1+r^3)^2} - \frac{2c_2r}{(1+r^2)^2} - \frac{c_1}{(1+r)^2}. \tag{50}$$

The system of equations obtained by substituting the conditions at the proposed function is:

$$\begin{cases} c_3 + c_2 + c_1 + \frac{c_0}{2} = 1, \\ \frac{c_3}{2} + \frac{c_2}{2} + \frac{c_1}{2} + \frac{c_0}{2} = 0, \\ c_1 = 0, \\ -\frac{3c_3}{4} - \frac{2c_2}{4} - \frac{c_1}{4} = 0. \end{cases} \tag{51}$$

Which results $c_0 = -2$, $c_1 = 0$, $c_2 = 6$, $c_3 = -4$.

The final expression of $I_3(r)$ is:

$$I_3(r) = -\frac{4}{1+r^3} + \frac{6}{1+r^2} - 1. \tag{52}$$

Function I_3 is shown at Figure 2, along with its first derivative.

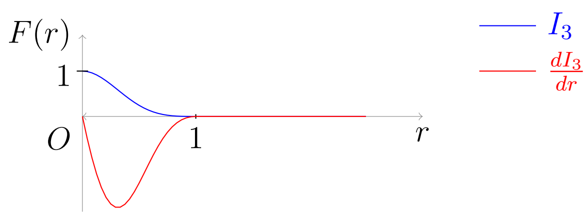

Figure 2: Graphical representation of function I_3.

Fourth Inverse Function

The next inverse function proposed is:

$$I_4(r) = \frac{c_4}{1+r^4} + \frac{c_3}{1+r^3} + \frac{c_2}{1+r^2} + \frac{c_1}{1+r} + \frac{c_0}{2}. \tag{53}$$

As before, to assure that the proposed function can serve well in the representation of continuous functions, the function will have to obey five conditions: $I_4(0) = 1$, $I_4(1) = 0$, $\frac{dI_4}{dr}\big|_{r=0} = 0$, $\frac{dI_4}{dr}\big|_{r=1} = 0$, and another condition that will have to be established in order to obtain the coefficients. This fifth condition, with respect to the second derivative of I_4, can either be:

$$\left.\frac{d^2 I_4^C}{dr^2}\right|_{r=0} = 0, \tag{54}$$

or

$$\left.\frac{d^2 I_4^S}{dr^2}\right|_{r=1} = 0. \tag{55}$$

The derivatives of I_4 can be obtained:

$$\frac{dI_4}{dr} = -\frac{4c_4 r^3}{(1+r^4)^2} - \frac{3c_3 r^2}{(1+r^3)^2} - \frac{2c_2 r}{(1+r^2)^2} - \frac{c_1}{(1+r)^2}, \tag{56}$$

and

$$\frac{d^2 I_4}{dr^2} = -4c_4\frac{3r^2 - 5r^6}{(1+r^4)^3} - 3c_3\frac{2r - 4r^4}{(1+r^3)^3} - 2c_2\frac{1-3r^2}{(1+r^2)^3} + c_1\frac{2}{(1+r)^3}. \tag{57}$$

When the curvature of the function vanishes either at the support radius ($r = 1$) the obtained equation is equivalent to the one already enforced for the first derivative. Therefore, there is no need to impose this condition to the function, or to add superscript C or S.

For the first condition, of null curvature at the origin ($r = 0$), the system of equations obtained is:

$$\begin{cases} c_4 + c_3 + c_2 + c_1 + \frac{c_0}{2} = 1, \\ \frac{c_4}{2} + \frac{c_3}{2} + \frac{c_2}{2} + \frac{c_1}{2} + \frac{c_0}{2} = 0, \\ c_1 = 0, \\ -c_4 - \frac{3c_3}{4} - \frac{2c_2}{4} - \frac{c_1}{4} = 0, \\ -2c_2 + 2c_1 = 0, \end{cases} \tag{58}$$

and the result of the system: $c_0 = -2, c_1 = 0, c_2 = 0, c_3 = 8, c_4 = -6$.

The final expression for $I_4(r)$ is:

$$I_4(r) = -\frac{6}{1+r^4} + \frac{8}{1+r^3} - 1. \tag{59}$$

Function I_4 is shown at Figure 3, along with its first and second derivatives. This function will also be tested against some of the well known CSRBFs.

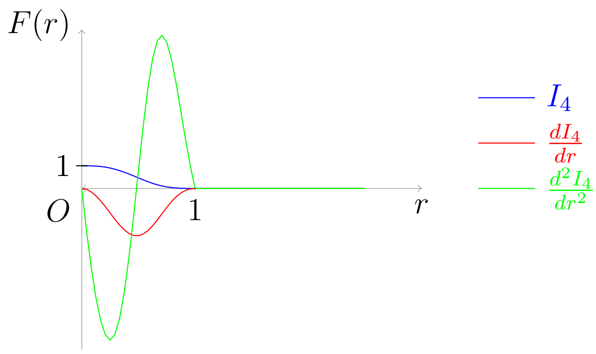

Figure 3: Graphical representation of function I_4.

Higher order inverse functions could easily be obtained, but this would unnecessarily increase the size of this paper. The reader is invited to more complete presentations in future publications.

On the next subsection, another family of functions is proposed.

3.2 Rational Functions

A rational function as proposed here is obtained by dividing two polynomials, the denominator being of the same order or one order higher than the numerator. Next the procedure for obtaining the coefficients shall be detailed.

$$R_{M/M} = \frac{\sum_{i=0}^{M} n_i r^i}{\sum_{j=0}^{M} d_j r^j}, \tag{60}$$

and

$$R_{M/M+1} = \frac{\sum_{i=0}^{M} n_i r^i}{\sum_{j=0}^{M+1} d_j r^j}. \tag{61}$$

The first of these functions, for $M = 1$, will be a continuous function, and can be set equal to the I_1 of Eq. 48.

The test functions proposed will be function $R_{3/3}$ and $R_{3/4}$, which will be obtained next.

Rational function of type 3/3

Defining the rational function of type 3/3, constructed by the ratio of two cubic polynomials:

$$R_{3/3}(r) = \frac{n_0 + n_1 r + n_2 r^2 + n_3 r^3}{d_0 + d_1 r + d_2 r^2 + d_3 r^3}. \tag{62}$$

The conditions for the function at $r = 0$ and at $r = 1$ are obtained after the derivatives.

For $r = 1$:

$$R_{3/3}(1) = 0 \quad \Rightarrow n_0 + n_1 + n_2 + n_3 = 0; \tag{63}$$
$$R'_{3/3}(1) = 0 \quad \Rightarrow n_1 + 2n_2 + 3n_3 = 0; \tag{64}$$
$$R''_{3/3}(1) = 0 \quad \Rightarrow 2n_2 + 6n_3 = 0; \tag{65}$$

and for $r = 0$:

$$R_{3/3}(0) = 1 \quad \Rightarrow n_0 = d_0; \tag{66}$$
$$R'_{3/3}(0) = 0 \quad \Rightarrow n_1 = d_1; \tag{67}$$
$$R''_{3/3}(0) = 0 \quad \Rightarrow n_2 = d_2. \tag{68}$$

Solving the above system of equations, it is obtained, from Eq. 63 (using Eq. 66), Eq. 64, and Eq. 65, $n_3 = -d_0$, $n_2 = 3d_0$ and $n_1 = -3d_0$. Thus results that, from Eq. 67, $d_1 = -3d_0$, and, from Eq. 68, $d_2 = 3d_0$.

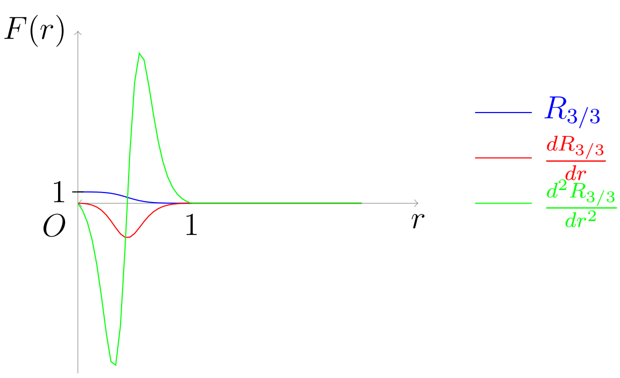

Figure 4: Graphical representation of function $R_{3/3}$.

Therefore:

$$R_{3/3}(r) = \frac{1 - 3r + 3r^2 - r^3}{1 - 3r + 3r^2 + r^3}, \tag{69}$$

where d_3 was arbitrarily set to unity ($d_3 = 1$).

The continuity of third derivatives cannot be guaranteed either at 0 or at 1. Figure 4 presents this function and its derivatives.

Rational function of type 3/4

Defining the rational function of type 3/4, constructed by dividing a cubic polynomial by a fourth order polynomial:

$$R_{3/4}(r) = \frac{n_0 + n_1 r + n_2 r^2 + n_3 r^3}{d_0 + d_1 r + d_2 r^2 + d_3 r^3 + d_4 r^4}. \tag{70}$$

The conditions for the function at $r = 0$ and at $r = 1$ are obtained after the derivatives.

For $r = 1$:

$$R_{3/4}(1) = 0 \quad \Rightarrow n_0 + n_1 + n_2 + n_3 = 0; \tag{71}$$
$$R'_{3/4}(1) = 0 \quad \Rightarrow n_1 + 2n_2 + 3n_3 = 0; \tag{72}$$
$$R''_{3/4}(1) = 0 \quad \Rightarrow 2n_2 + 6n_3 = 0; (i-6)*(6+21*i-15*i^2)*r^(2*i-4) \tag{73}$$

and for $r = 0$:

$$R_{3/4}(0) = 1 \quad \Rightarrow n_0 = d_0; \tag{74}$$
$$R'_{3/4}(0) = 0 \quad \Rightarrow n_1 = d_1; \tag{75}$$
$$R''_{3/4}(0) = 0 \quad \Rightarrow n_2 = d_2; \tag{76}$$
$$R'''_{3/4}(0) = 0 \quad \Rightarrow n_3 = d_3. \tag{77}$$

Solving the above system of equations, it is obtained, from Eq. 71 (using Eq. 74), Eq. 72, and Eq. 73, $n_3 = -d_0$, $n_2 = 3d_0$ and $n_1 = -3d_0$. Thus results that, from Eq. 75, $d_1 = -3d_0$, from Eq. 76, $d_2 = 3d_0$, and, from Eq. 77, $d_3 = -d_0$.

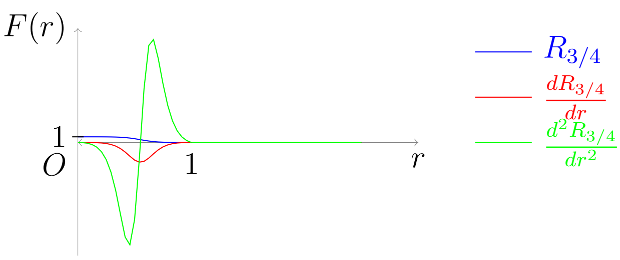

Figure 5: Graphical representation of function $R_{3/4}$.

Therefore:

$$R_{3/4}(r) = \frac{1 - 3r + 3r^2 - r^3}{1 - 3r + 3r^2 - r^3 + r_4}, \tag{78}$$

where d_4 was arbitrarily set to unity ($d_4 = 1$).

The continuity of the third derivative cannot be guaranteed at 1, or of fourth derivative for either the center or the support radius. Figure 5 presents this function and its derivatives.

3.3 Summary of Proposed functions

Although only the derivation of the first function and of the ones used is presented, it is though that a more complete set should be presented. To summarize the proposed functions Tables 4 and 5 are presented. In these tables the continuity properties are given for each function.

Table 4: Inverse functions and continuity.

Function	Continuity	Observation
$I_1(r) = \frac{2}{1+r} - 1$	C^0	
$I_2^C(r) = \frac{2}{1+r^2} - 1$	C^0	Center
$I_2^S(r) = -\frac{2}{1+r^2} + \frac{4}{1+r} - 1$	C^0	Support
$I_3(r) = -\frac{4}{1+r^3} + \frac{6}{1+r^2} - 1$	C^1	
$I_4(r) = -\frac{6}{1+r^4} + \frac{8}{1+r^3} - 1$	C^2	
$I_5^C(r) = -\frac{8}{1+r^5} + \frac{10}{1+r^4} - 1$	C^2	Center
$I_5^S(r) = \frac{7}{1+r^5} - \frac{20}{1+r^4} + \frac{15}{1+r^3} - 1$	C^2	Support

Center - The next higher derivative is continuous at the center ($r = 0$).

Support - The next higher derivative is continuous at the support radius ($r = 1$).

4 RESULTS

In order to investigate the behaviour of these novel kinds of proposed functions, the solution of a simple heat conduction problem is attempted with a simple least squares meshfree finite element code (Menandro et al., 2011) using some of the classic CSRBFs and some of the proposed CSRBFs.

The problem to be solved is an L-shaped plate (1×1) with prescribed temperature functions on two sides and vanishing heat flux on the other faces.

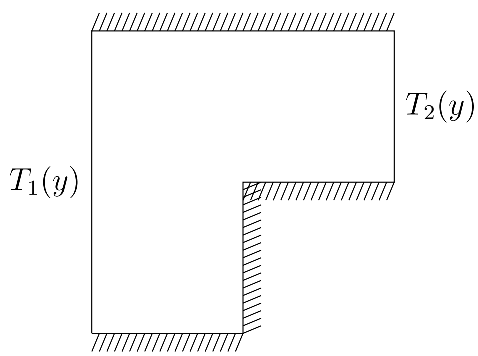

Figure 6: Test problem - L-shaped heat conduction.

Figure 6 shows the sample problem tested. Prescribed temperature $T_1(y) = 6.5 - 3.5y$, at face 1, is linearly distributed along the face and evaluates to $T_1 = 6.5°C$ at the bottom side and

Table 5: Rational functions and continuity.

Function	Continuity	Observation
$R_{1/1}(r) = \frac{1-r}{1+r}$	C^0	
$R_{1/2}(r) = \frac{2-2r}{2-2r+r^2}$	C^0	Center
$R_{2/2}(r) = \frac{1-2r+r^2}{1-2r+2r^2}$	C^1	
$R_{2/3}(r) = \frac{1-2r+r^2}{1-2r+r^2+r^3}$	C^1	Center
$R_{3/3}(r) = \frac{1-3r+3r^2-r^3}{1-3r+3r^2+r^3}$	C^2	
$R_{3/4}(r) = \frac{1-3r+3r^2-r^3}{1-3r+3r^2-r^3+r_4}$	C^2	Center
$R_{4/4}(r) = \frac{1-4r+6r^2-4r^3+r^4}{1-4r+6r^2-4r^3+2r_4}$	C^3	
$R_{4/5}(r) = \frac{1-4r+6r^2-4r^3+r^4}{1-4r+6r^2-4r^3+r^4+r^5}$	C^3	Center
$R_{5/5}(r) = \frac{1-5r+10r^2-10r^3+5r^4-r^5}{1-5r+10r^2-10r^3+5r^4+r^5}$	C^4	

Center - The next higher derivative is continuous at the center ($r = 0$).

$T_1 = 3.0°C$ at the top. Face 2 also presents linearly varying prescribed temperature, from seven to fourteen degrees Celsius, $T_2(y) = 14.0y$.

To compare the accuracy and convergence of the proposed functions the solution is obtained for Wendland functions of C^2 and C^4 continuity which are positive definite on $\mathbb{R}^3$ (Eq. 16 and 17), Wu functions of the same characteristics (Eq. 29 and 31), and four of the proposed functions. The two inverse functions are the I_3 (Eq. 52) and I_4 functions (Eq. 59). The first is a C^1 continuous function and the second a C^2 continuous function. The two rational functions used are the $R_{3/3}$ (Eq. 69) and $R_{3/4}$ functions (Eq. 78). The first is a C^2 continuous function and the second is also continuous, with continuous first and second derivatives, but also has a continuous third derivative at $r = 0$.

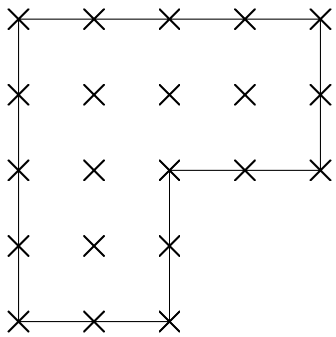

Figure 7: Cloud of 21 points.

The problem is modelled using clouds of squarely distributed function center points, using 21, 40, 65, 96, 133, 176, 225, and 280 functions. As can be seen at Fig. 7, for 21 points there are 5 points on face 1: for the other point clouds there are, respectively, 7, 9, 11, 13, 15, 17, and 19 points on face 1. The discrete least squares procedure (Menandro et al., 2011) is performed using 936 squarely distributed evaluation points (35 points on face 1). The boundary conditions are enforced at 31 boundary points, eleven of them for the prescribed temperature faces (Dirichlet conditions) and 21 for the Neumann prescribed heat flux (adiabatic) conditions. The Boundary conditions are enforced through a Lagrange multiplier procedure on the resulting system of equations. After the calculation is performed for each function, the normalized root mean squared error is estimated as the root mean residue of the differential equation, summed over all the evaluation points, and normalized by the amplitude of the calculated response.

Table 6: Root mean square residue error for Wendland and Wu functions

Functions	Wendland $C^2\ PD^3$	Wendland $C^4\ PD^3$	Wu $C^2\ PD^3$	Wu $C^4\ PD^3$
21	109.347000	935.325000	104.332000	389.509000
40	25.288000	149.411000	10.193800	50.113200
65	2.848650	3.017790	2.456160	2.573300
96	2.442350	2.342090	2.200940	2.546230
133	2.242170	2.002040	1.929780	1.628330
176	2.088630	1.828500	1.777020	1.621540
225	2.004730	1.738950	1.694630	1.601460
280	1.923930	1.703340	1.622820	1.699910

The results for the functions proposed by Wendland (1995) and Wu (1995) are shown at Table 6. The slight divergence for the later function, Wu $C^4\ PD^3$, for 280 approximating functions should be observed. This could be interpreted as a limit for the discrete least squares procedure (in other problems, as the number of evaluation points increases this apparent divergence disappears).

Table 7: Root mean square residue error for the novel functions

Functions	I_3	I_4	$R_{3/3}$	$R_{3/4}$
21	5644.400000	5.814340	43.348500	38.650000
40	11.256400	4.742550	2.416280	3.873640
65	2.297720	3.257690	1.463530	2.556680
96	2.228320	1.396630	1.156910	1.190820
133	1.577010	1.327770	0.981073	1.250140
176	1.499410	1.317880	0.931537	1.208960
225	1.448520	1.293130	0.947840	1.729350
280	1.399820	1.258720	0.941966	2.132290

The results for the proposed functions are shown at Table 7. Again, the apparent divergent behaviour is observed for both Rational functions (both functions $R_{3/3}$ and $R_{3/4}$ present higher error for 225 and 280 approximating RBFs than for 176 functions, though for the first the residue error seems to continue to decrease).

Both results shown at Tables 6 and 7 are presented at Fig. 8. The residue error values are plotted against the number of approximating functions using logarithmic scales in an attempt to capture the convergence rates of the chosen method for each of the tested functions.

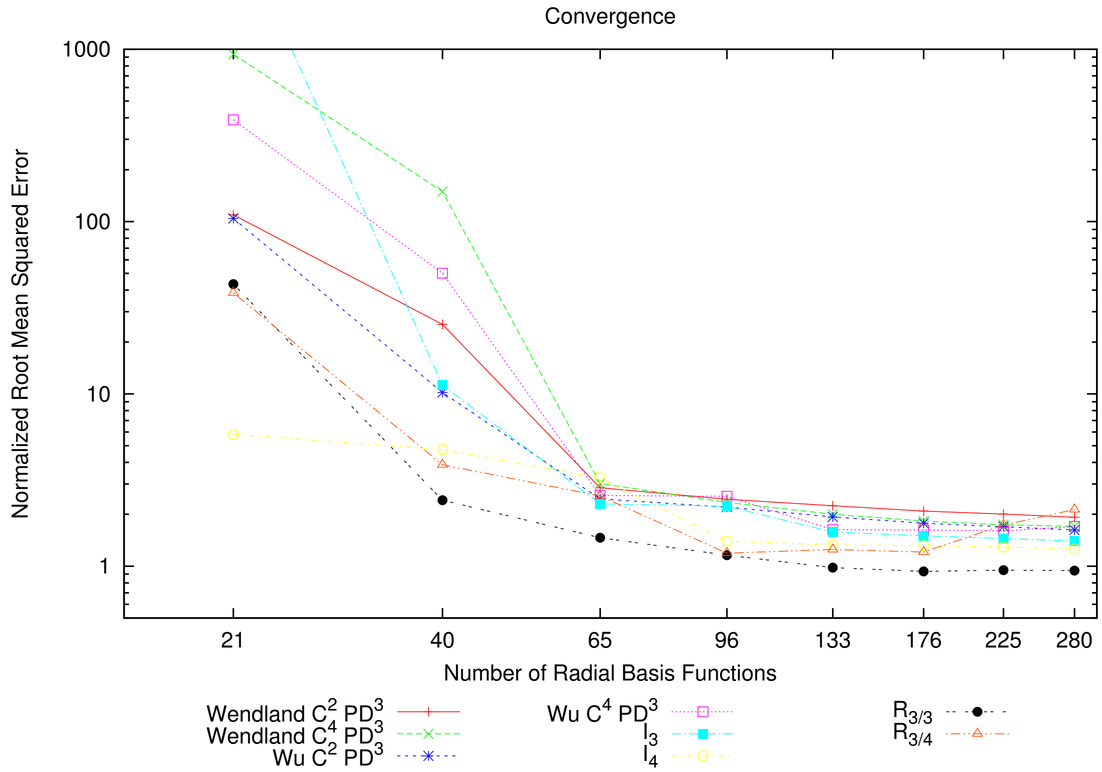

Figure 8: Root mean squared error of residue for the test problem.

The convergence rate is calculated by linear regression for each of the tested functions assuming a negative power law for the error function:

$$\varepsilon(N_{RBF}) = A\,(N_{RBF})^{-B}\,, \tag{79}$$

where A is a mathematical parameter corresponding to a possible solution with one approximating function, B is the convergence rate, ε is the normalized root mean squared residue error, and N_{RBF} is the number of Radial Basis Functions.

The calculated parameters for the given data are shown at Table 8.

As can be observed at Table 8, the first parameter seems to diverge for the given results, which can be accounted for an incapacity of the given cloud point set to accurately approximate the solution response. The only exception is for the I_4 function, and is observable at Fig. 8 and on the temperature plot for this approximation (Fig. 9). Even though the temperature distribution is not strictly correct, it is a fair approximation, as the error is only 5.81434% of the

Table 8: Convergence parameters for the tested functions.

Functions	A	B
Wendland C^2 PD^3	166261 $\pm$ 6.833e+04	2.40605 $\pm$ 0.1338
Wendland C^4 PD^3	8.45537e+06 $\pm$ 3.647e+06	2.99177 $\pm$ 0.1416
Wu C^2 PD^3	4.97436e+06 $\pm$ 3.349e+06	3.53832 $\pm$ 0.2218
Wu C^4 PD^3	8.02762e+06 $\pm$ 2.482e+06	3.26264 $\pm$ 0.1017
I_3	2.36171e+13 $\pm$ 3.665e+13	7.27721 $\pm$ 0.5153
I_4	49.7368 $\pm$ 16.04	0.686288 $\pm$ 0.0875
$R_{3/3}$	1.77246e+07 $\pm$ 2.971e+07	4.24469 $\pm$ 0.5537
$R_{3/4}$	805738 $\pm$ 1.183e+06	3.26694 $\pm$ 0.4827

temperature amplitude (Table 7). With respect to the convergence rate B, it is observed that the values for the proposed functions are not quite distant from those for well accepted CSRBFs.

If the initial incapacity for interpolation is not taken into the convergence calculations, as well as the latter apparent divergence, the convergence parameters could be calculated for 65, 96, 133, and 176 approximating RBFs. This is the linear part of Fig. 8. This results are shown at Table 9

Table 9: Recomputed convergence parameters for the tested functions.

Functions	A	B
Wendland C^2 PD^3	10.5319 $\pm$ 1.261	0.315679 $\pm$ 0.02589
Wendland C^4 PD^3	26.9038 $\pm$ 6.109	0.527704 $\pm$ 0.04976
Wu C^2 PD^3	9.79107 $\pm$ 0.7795	0.330088 $\pm$ 0.01723
Wu C^4 PD^3	23.4412 $\pm$ 21.06	0.517928 $\pm$ 0.1968
I_3	16.448 $\pm$ 10.78	0.462232 $\pm$ 0.1431
I_4	459.455 $\pm$ 801.3	1.20035 $\pm$ 0.3966
$R_{3/3}$	11.0368 $\pm$ 2.985	0.487898 $\pm$ 0.05913
$R_{3/4}$	118.839 $\pm$ 194.1	0.937765 $\pm$ 0.3666

For the new values of the convergence parameters it is observed that the I_3 and $R_{3/3}$ functions produce very similar convergence functions ε as those for Wendland or Wu functions. For the other two proposed test functions, the convergence rate also has a similar order of magnitude, but the first parameter increases due to the specific characteristics of the results. It should be noted that the standard deviation is higher than the computed value, for both I_4 and $R_{3/4}$ functions. This occurs due to the small number of sample analyses utilized and, to a certain extent, can also be observed for the Wu C^4 PD^3 function, where the standard deviation is of

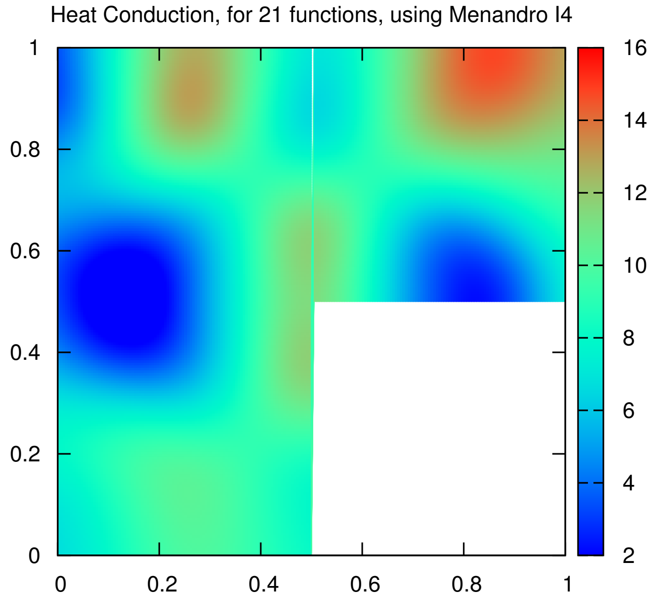

Figure 9: Temperature plot for test problem, with 21 I_4 approximating functions.

the same order of magnitude as the value of the A parameter.

Finally, a temperature plot for 225 I_4 points is shown at Fig. 10, showing the convergence of the proposed solution to the correct solution.

5 FINAL REMARKS

The proposed sets of functions, when compared to two well accepted CSRBF kinds, present similar convergence parameters. The convergence rates are, in general, higher than those obtained for the tested classical functions. These results confirm the initial hypothesis that the proposed classes of CSRBFs can be used to correctly approximate the solution of differential equations: not only the estimated error for most of the analyses performed was similar, but the convergence rate also returns comparable values.

These results confirm that the proposed functions perform well for the solution of differential equations by a discrete least squares evaluation, as long as the number of approximation functions is sufficient (for a squarely distributed function center cloud) and the number of least squares discrete evaluation points is enough to capture the peculiarities of the specific point cloud.

The results also demand more work on the mathematical properties of the proposed classes of functions, such as the complete definition of their positive definiteness dimensionality, for this is an essential property towards a completeness of solution and mathematical convergence proof.

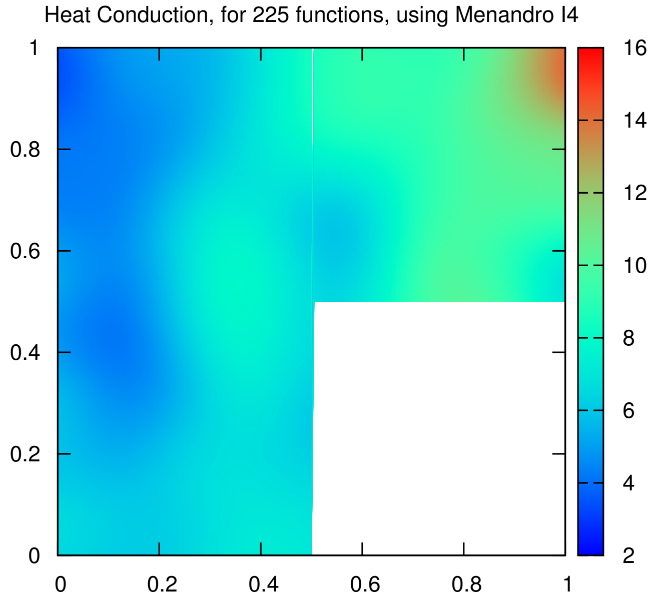

Figure 10: Temperature plot for test problem, with 225 I_4 approximating functions.

REFERENCES

Belytschko, T., Y. Krongauz, D. Organ, M. Fleming, and P. Krysl, 1996. Meshless methods: an overview and recent developments. *Comput. Methods Appl. Mech. Engrg. 139*, pp. 3–47.

Buhmann, M. D., 1998. Radial functions on compact support. *Proceedings of the Edinburgh Mathematical Society 41*, pp. 33–46.

de Boer, A., M. S. van der Schoot, and H. Bijl, 2007. Mesh deformation based on radial basis function interpolation. *Computers and Structures 85*, pp. 784–795.

Fasshauer, G. E., 2007. *Meshfree Approximation Methods with MATLAB*. World Scientific.

Floater, M. S. and A. Iske, 1996. Multistep scattered data interpolation using compactly supported radial basis functions. *Journal of Computational and Applied Mathematics 73*, pp. 65–78.

Gaspari, G. and S. E. Cohn, 1999. Construction of correlation functions in two and three dimensions. *Quarterly Journal of the Royal Meteorological Society 125*(554), pp. 723–757.

Gneiting, T., 2002. Compactly supported correlation functions. *Journal of Multivariate Analysis 83*(2), pp. 493 – 508.

Goldberg, M. A., C. S. Chen, and H. Bowman, 1999. Some recent proposals for the use of radial basis functions in the bem. *Engineering Analysis with Boundary Elements 23*, pp. 285–296.

Hickernell, F. J. and Y. C. Hon, 1999. Radial basis function approximations as smoothing splines. *Applied Mathematics and Computation 102*, pp. 1–24.

Hubert, S., 2012. Closed form representations for a class of compactly supported radial basis functions. *Adv. Comput. Math. 36*, pp. 115–136.

Iske, A., 2004. *Multiresolution Methods in Scattered Data Modelling*. Springer.

Menandro, F. C. M., C. F. Loeffler Neto, and A. Bulcao, 2011. Function interpolation using compactly supported radial basis functions: a geophysical application. In *Proceedings of the XXVI CILAMCE*.

Menandro, F. C. M., H. J. S. G. Meira, and C. F. Loeffler Neto, 2011. Meshfree finite element solution of differential equations by radial basis functions interpolation. In *Proceedings of the XXVI CILAMCE*.

Moreaux, G., 2008. Compactly supported radial covariance functions. *Journal of Geodesy 82*(7), pp. 431–443.

Schaback, R., 1995. Creating surfaces from scattered data using radial basis functions. In *in Mathematical Methods for Curves and Surfaces*, pp. 477–496. University Press.

Wendland, H., 1995. Piecewise polynomial, positive definite and compactly supported radial functions of minimal degree. *Adv. Comput. Math. 4*, pp. 389–396.

Wendland, H., 1996. *Konstruktion und Untersuchung radialer Basisfunktionen mit kompaktem Träger*. Ph. D. thesis, Georg-August-Universität zu Göttingen.

Wendland, H., 2005. *Scattered Data Approximation*. Cambridge University Press.

Wong, S. M., Y. Hon, and M. A. Goldberg, 2002. Compactly supported radial basis functions for shallow water equations. *Applied Mathematics and Computation 127*, pp. 79–101.

Wu, Z., 1995. Compactly supported positive definite radial functions. *Adv. Comput. Math. 4*, pp. 283–292.

Zhu, S., 2012. Compactly supported radial basis functions: how and why? *SIAM Review*.